

Experimental Study of High-efficiency Single-stage 30 K Coaxial Pulse Tube Cryocooler

Yanen Li ^{1,2}, Nailiang Wang ^{1,*}, Miguang Zhao ^{1,*}, GuoPeng Wang ¹, Min Gao ^{1,2}, Bin Yang ^{1,2}, Geyang Li ^{1,2} and Ye Yuan ^{1,2}

¹ Key Laboratory of Technology on Space Energy Conversion, Technical Institute of Physics and Chemistry, Chinese Academy of Science, Beijing, China

² University of Chinese Academy of Sciences, Beijing, China

*E-mail: wangnl@mail.ipc.ac.cn, mgzhao@mail.ipc.ac.cn

Abstract. The operating temperature of 30 K is crucial for long-wave infrared and very long-wave infrared detectors. To achieve cooling at 30 K, a two-stage pulse tube cryocooler (PTC) has been employed in most previous studies. However, these systems are complex in structure. Single-stage 30 K high-efficiency PTC developments present significant challenges but are essential for 30 K long-wave infrared detectors. We designed a single-stage coaxial PTC with a double inlet orifice and conducted extensive optimization experiments on this cryocooler. With 200 W input power and a hot end temperature of 285 K, the PTC achieved a cooling capacity of 1.6 W/30 K, corresponding to a relative Carnot efficiency of 6.8%.

1. Introduction

To achieve higher resolution and reliability, space infrared detectors require low-temperature operation to minimize dark current. The operational temperature of the detector's core components decreases with longer detected wavelengths. An operation temperature of 30 K is crucial for long-wave infrared (LWIR, 6–15 μm) and very long-wave infrared (VLWIR, 15–30 μm) detectors.

Many scholars have conducted extensive research on 30 K PTCs. To achieve cooling at 30 K efficiently, most 30 K PTCs adopt a two-stage structure ^[1-5]. The two-stage PTC is considerably more complex than a single-stage cryocooler design for space applications. Consequently, achieving efficient cooling at 30 K using a single-stage PTC has become a burgeoning research focus.

With PTC technology's continuous development and maturation, single-stage designs have also achieved temperatures below 30 K without load, providing significant cooling at 30 K. In 1995, TRW^[6] reported a single-stage PTC achieving a minimum temperature of 29.2 K, delivering 1 W of cooling power at 35 K with an input power of 200 W. In 2010, Yang^[7] achieved a minimum temperature of 26.1 K with an input power of 250 W in their research on cryocoolers operating below 30 K. At 200 W input power, the cryocooler provided cooling power ranging from 0.3 W to 0.5 W at 35 K. In 2018, Chen^[8] implemented a multi-bypass and double inlet structure in their PTC, achieving a minimum temperature of 15.5 K at 246 W input power. They obtained 386 mW of cooling power at 20 K and nearly 1.5 W at 30 K. After further improvements to the filling matrix of the regenerator, they achieved a record low temperature of 13.9 K for a single-stage PTC at 250 W input power, providing nearly 0.8 W of cooling power at 30 K^[9]. In 2018, Liu^[10] developed a



single-stage PTC, achieving a minimum temperature of 24.4 K, with the cryocooler delivering 1 W of cooling performance at 30 K with an input power of 227 W.

To meet the requirements of space infrared detectors operating at 30 K, this study aims to design a PTC that operates efficiently at 30 K while providing significant cooling capacity. In our experimental research, we chose the optimal cold finger. We selected the appropriate diameter of the double inlet orifice. Once the basic structure of the cryocooler was determined, we conducted experiments to assess its operational parameters and measured its cooling performance. At an input power of 200 W, the cryocooler achieved a no-load temperature of 18.6 K and provided cooling capacities of 1.6 W at 30 K or 3.1 W at 40 K.

2. Experimental System

The PTC consists of four main components: a compressor, a hot-end heat exchanger, a cold finger, and a phase shifter. The compressor is a linear motor-driven piston compressor with an opposed piston arrangement. The slit-type hot-end heat exchanger is designed to dissipate most of the heat generated by the cryocooler. External cooling is provided to the hot-end heat exchanger using cooling water. The cryocooler's cold finger utilizes a coaxial arrangement with a regenerator filled with stainless steel wire mesh. At the cold end, a copper slit-type heat exchanger allows extraction and utilization of the cooling capacity. Temperature measurement of the cryocooler is performed using Lakeshore diode temperature sensors, and cooling capacity is measured using the heat balance method.

The inertance tube and reservoir were employed as a phase shifter. Additionally, the structure of a double-inlet orifice is used, with a small hole at the hot end of the pulse tube serving as a double-inlet orifice.

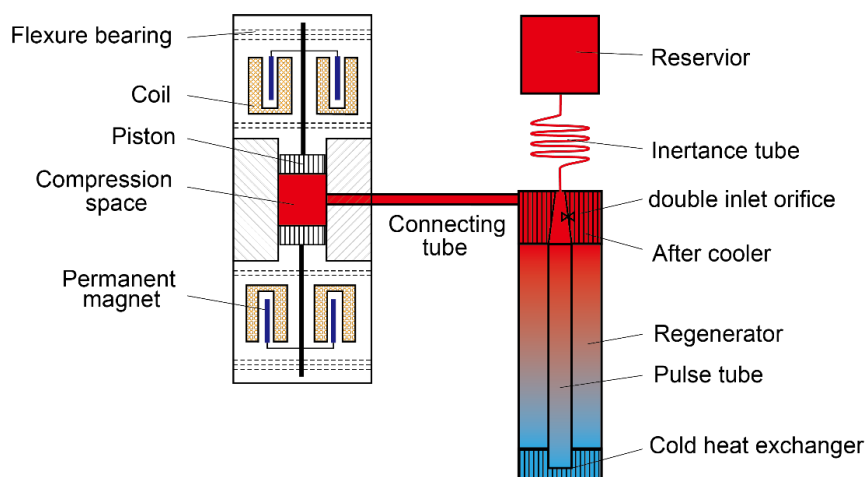


Figure 1. Schematic diagram of the PTC with double inlet orifice.

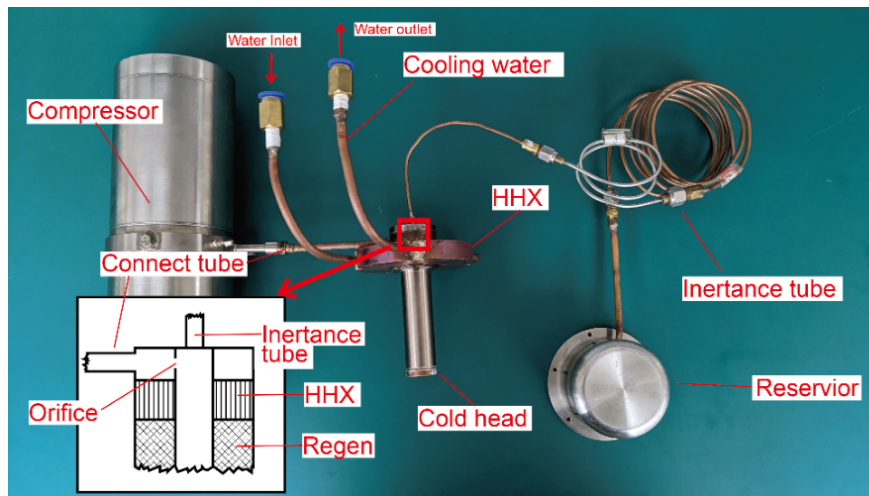


Figure 2. Actual picture of the 30 K single-stage PTC.

3. Experimental Results and Analysis

In the experiments, we tested the performance of different cold fingers to identify the optimal cold finger. Subsequently, to achieve a lower no-load temperature for the cryocooler, we explored the impact of various diameters of double inlet orifice on the performance of PTC. Through these optimization experiments, we finalized the basic structure of the cryocooler and conducted performance tests.

3.1 Performance of different cold fingers

In the experiment, we manufactured three different cold fingers and conducted tests with parameters as shown in Table 1. 500-mesh or 600-mesh stainless steel wire mesh was used for regenerator filling, and three cold fingers were filled using different methods. Compared to the 500-mesh wire mesh, the 600-mesh wire mesh has minor porosity and wire diameter, allowing for more effective heat transfer but also resulting in higher flow resistance. PTC's performance with different cold fingers was measured, and the results are shown in Figure 3. Cold fingers 2 and 3 exhibited poorer performance than cold finger 1, likely due to the higher flow resistance

Table 1. Key parameters of different cold fingers

Number	Length of regen	Matrix mesh
Cold finger 1	80 mm	500# SS, porosity 0.613, filling length 80 mm
Cold finger 2	80 mm	500# SS, porosity 0.613, filling length 40 mm 635# SS, porosity 0.606, filling length 40 mm
Cold finger 3	90 mm	500# SS, porosity 0.613, filling length 45 mm 635# SS, porosity 0.606, filling length 45 mm

^a The inner and outer diameter of the regenerator are respectively as 25 mm and 10.7 mm.

introduced by the 600# SS matrix. Therefore, cold finger 1 was considered the optimal cold finger and used for 30 K PTC.

3.2. Performance of different double inlet orifice

In the above experiments, a 0.4 mm diameter double inlet orifice was drilled at the hot end of the cold finger to connect the hot end of the regenerator and pulse tube. To investigate the effect of different hole diameters on the cryocooler's performance, we compared the impact of various double inlet orifice diameters on cryocooler performance, as shown in Figure 4. The double inlet orifice's diameter affects the mass flow rate through the orifice, influencing the cryocooler's performance. A larger diameter orifice allows for a more extensive mass flow bypass, resulting in a higher DC flow in the PTC.

The performance curves of the cryocooler with different diameters of double inlet orifice are shown in Figure 4. The performance of the PTC with a 0.2 mm diameter orifice and the PTC without an orifice (diameter equals 0) overlap, indicating similar performance. The PTC with a 0.4 mm diameter orifice demonstrates excellent performance, while huge orifice diameters can introduce excessive DC flow into the cryocooler. Therefore, we chose a double inlet orifice with a

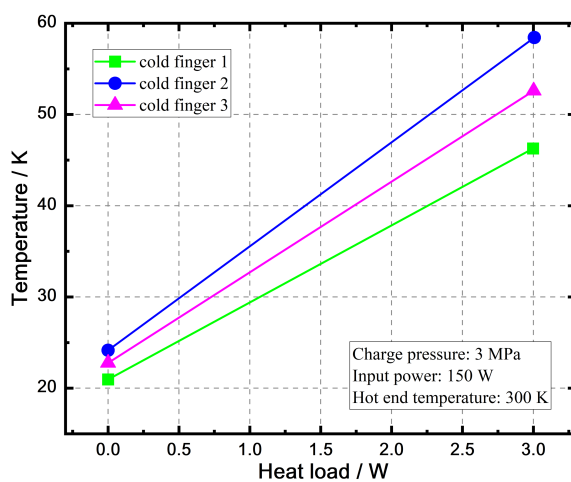


Figure 3. Performance of PTC with different cold fingers.

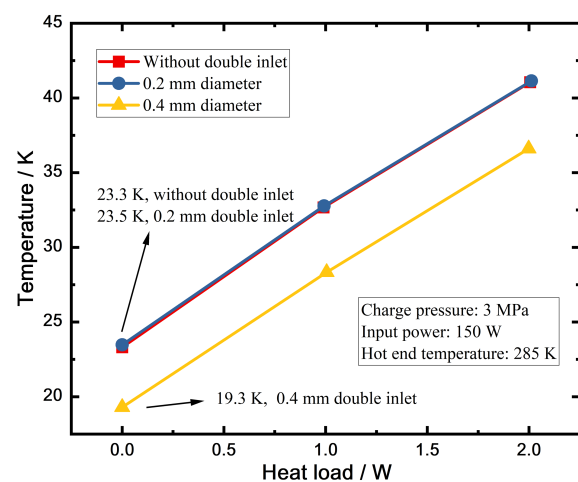


Figure 4. Performance of PTC with different double inlet orifice diameters.

0.4 mm diameter. Furthermore, by reducing the temperature of the cryocooler's hot end from an ambient temperature of 300 K to 285 K, we observed a decrease in the no-load temperature achievable to 19.3 K.

3.3 Performance of the 30 K PTC

We have established the cryocooler's basic structure and operating conditions through optimization. The cryocooler's key parameters and operating conditions are summarized in Table 2. Additionally, we measured the performance of the cryocooler with different input electrical power, as depicted in Figure 5.

Notably, at an input power of 200 W, the PTC achieved a no-load temperature of 18.7 K. At temperatures of 30 K and 40 K, it provided cooling capacities of 1.6 W and 3.1 W, respectively, corresponding to relative Carnot efficiencies of 6.8% and 9.5%. When the input power was reduced to 150 W, the cooling curve is depicted in Figure 6. The cold head temperature decreased

from room temperature (300 K) to 40 K in 16 minutes and reached a steady no-load temperature of 19.3 K after 67 minutes.

Table 3. Key parameters of the 30 K PTC

Component	Parameters	Values
Compressor	diameter of piston	25 mm
	swept volume, compression ratio	9.6 cc, 1.27
Connecting tube	length and diameter	100 mm, 6 mm
Cold finger	Length and diameter of regen	80 mm, 25 mm
	diameter of pulse tube*	10.7 mm
	matrix	500# SS wire screen, porosity 0.613
Operation	charge pressure, frequency	3 MPa, 36 Hz

* In the coaxial configuration, the inner diameter of regenerator matches the outer diameter of pulse tube.

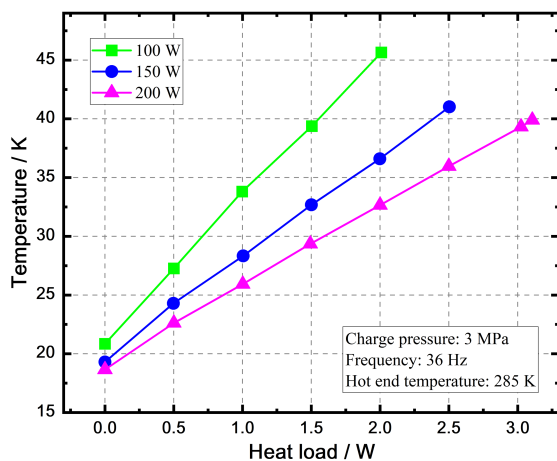


Figure 5. Performance of the 30 K PTC.

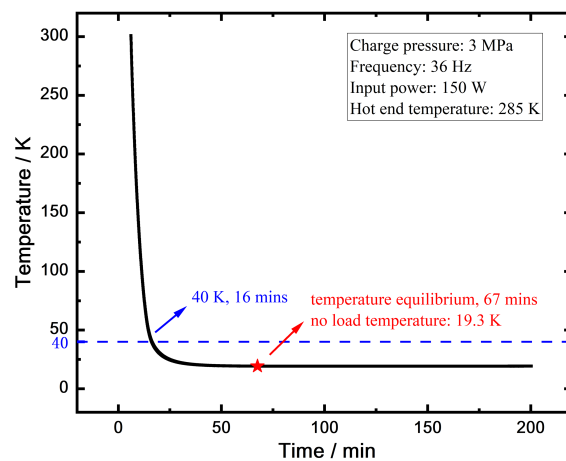


Figure 6. Cooling curve of the 30 K PTC.

4. Conclusion

In our study, we conducted tests and optimizations on cold fingers. We experimented with different diameters of double inlet orifice to determine the optimal size. Following optimizations and confirming the fundamental structure of the cryocooler, we tested its critical performance. With an input electrical power of 200 W, we achieved a no-load cooling temperature of 18.6 K. We obtained cooling capacities of 1.6 W at 30 K or 3.1 W at 40 K, with relative Carnot efficiencies of 6.8% or 9.5%.

References

- [1] Prouvé T, Charles I, Leenders H, Mullié J, Tanchon J, Trollier T. and Tirolien T. 2016 Progress on 30K-50K Two-Stage EM PT Cold Finger for Space Applications
- [2] Yang, L. 2008 Investigation on a thermal-coupled two-stage Stirling-type pulse tube cryocooler *Cryogenics* **48(11-12)** pp.492-496.
- [3] Sun D. M., Dietrich M., Thummes G. 2009 High-Power Stirling-Type Pulse Tube Cooler Working below 30K *Cryogenics* **49 (9)** 457–462(<https://doi.org/10.1016/j.cryogenics.2009.06.006>)
- [4] Charles I, Coynel A, Duval J, Daniel C, Briet R 2009 Development of a Two-Stage High-Temperature Pulse Tube Cooler for Space Applications in *Proc. of 15th ICC*
- [5] Gully W, Glaister D, Hendershott P, Kotsubo V, Lock J, Marquardt E. 2007 Ball Aerospace Next Generation Two-Stage 35 K Coolers: The SB235 and SB235E *International Cryocooler Conference*
- [6] Burt W, Chan C. 1995 Demonstration of a High Performance 35 K Pulse Tube Cryocooler *In Cryocoolers 8* (pp. 313-319) Boston MA: Springer US (https://doi.org/10.1007/978-1-4757-9888-3_31)
- [7] Yang L. W., Xun Y. Q., Thummes G., Liang J. T. 2010 Single-Stage High-Frequency Coaxial Pulse Tube Cryocooler with Base Temperature below 30K *Cryogenics* **50(5)** pp.342-346 (<https://doi.org/10.1016/j.cryogenics.2010.01.009>.)
- [8] Chen L., Zhou Q., Jin H., Zhu W., Wang J., Zhou Y. 2013 386mW/20K Single-Stage Stirling-Type Pulse Tube Cryocooler *Cryogenics* **57** pp.195-199 (<https://doi.org/10.1016/j.cryogenics.2013.03.004>)
- [9] Zhou Q., Chen L., Zhu X., Zhu W., Zhou Y., Wang J. 2015 Development of a High-Frequency Coaxial Multi-Bypass Pulse Tube Refrigerator below 14K *Cryogenics* **67** pp.28-30. (<https://doi.org/10.1016/j.cryogenics.2015.01.006>.)
- [10] Liu S. S., Jiang Z. H.; Zhang A. K., Tang Z. G., Ding L., Wu Y. N. 2018 Study on high energy efficiency 30 K single-stage pulse tube cryocooler for a space infrared detector *J. Infrared Millim. Waves* **37(4)** pp.403-410 (<https://doi.org/10.11972/j.issn.1001-9014.2018.04.005>)

Acknowledgments

This work was Supported by the National Natural Science Foundation of China Grant No. 52106036 and the Scientific Instrument Developing Project of the Chinese Academy of Sciences, Grant No. ZDKYYQ20220004.